Dynamic Filtering of Stochastic Solar Resources Using HVAC Drive Control – A Determination of Feasible Bandwidth

Yue Cao, John A. Magerko III, Thomas Navidi, *Student Member*, *IEEE*,
Philip T. Krein[1], *Fellow*, *IEEE*

***Abstract*—This paper defines a bandwidth over which power electronic HVAC (heating, ventilation, and air-conditioning) drives can operate such that when integrated with stochastic solar power they act as an effective electric swing bus to mitigate solar power variability. In doing so, grid power is shown to be substantially more constant, reducing the need for fast grid resources or dedicated energy storage. The concept is equivalent to using building thermal energy as virtual dynamic storage in support of power grid operation. Two years of solar data have been collected on sub-millisecond time scales to test the results. Here a three-day sample is used to evaluate efficacy, determine solar frequency-domain content, and test a low-pass filtering concept introduced to model ideal power compensation. A more practical band-pass filter is realized that provides 1) lower frequency bounds such that the building maintains consistent room temperature via the HVAC system as demonstrated by a thermal modeling study, and 2) upper frequency bounds that ensure commanded HVAC fan speeds do not update arbitrarily fast. The latter primarily avoids acoustic discomfort to users. The combination is illustrated by experimental results based on various update rates of a variable frequency fan drive over a sample of actual stochastic solar data.**

***Index Terms*—Energy efficient buildings, frequency domain analysis, grid-level energy storage, HVAC systems, solar energy, thermal storage, power electronic drives**

I. Introduction

Energy-efficient buildings, including several net-zero energy commercial buildings, have been constructed around the globe. Research activities on this topic have increased in recent years [1-4], and many occupants have shown interest in having net-zero energy buildings as their future offices such as the new Apple "Spaceship" in Cupertino, California [5]. Energy efficient or net-zero energy buildings often include onsite photovoltaic (PV) solar panels. These panels provide non-constant power that can vary rapidly, due to weather conditions, local intermittent shading, passing clouds or flocks of birds, differential soiling, and time of day. Considering this inconstancy to represent an unwanted ac signal from a PV system, a suitable filter could be implemented but would require storage. Although the most familiar challenge is the full diurnal solar cycle (imposing substantial energy storage requirements for evening and night loads), rapid dynamic changes in solar energy are more difficult to address. Batteries or supercapacitor banks are often discussed [6-8]. If instead one utilizes the thermal storage capacity or thermal inertia inherent in a building, then HVAC (heating, ventilation, and air-conditioning) system adjustment can implement electrical storage, much like an electric swing bus [9-13]. Such an electric swing bus could offset fast variations of local solar power from a grid perspective with reduced need for conventional storage. The scaling potential is sizeable, given that nearly 40% of annual U.S. energy is consumed in residential and commercial buildings [14] with nearly half of that consumed by HVAC systems [15].

We will demonstrate how intelligent control of HVAC drives can compensate, within predetermined frequency and amplitude limit, for onsite solar power over short time intervals without disrupting building temperature and comfort. The process is based on concepts in [9-11]. In particular, [9] shows how bandwidth concepts can take advantage of HVAC dynamic adjustment to offset energy resource variability. Power electronics enables this control via dc-dc converters, inverter-based drives, and other existing hardware, as illustrated in Figure 1. The results formally take advantage of thermal energy storage, but in this paper the emphasis is on mitigating fast dynamic variability, more akin to treating HVAC as accessing thermal inertia. Utilizing thermal inertia can alleviate the need for inherently expensive, fast-varying, grid-side (or building-side) resources. This is nearly equivalent to placing a low-pass filter on a building's net generation and usage, requiring grid-side assistance only when changes in load-side demand persist beyond an extended interval [16]. Given the slow thermal response of a building, we might anticipate that times scales of a few minutes or faster can be used to advantage to offset resource variability without noticeable impact on occupants.

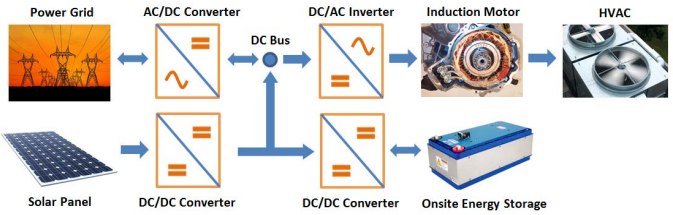

Figure 1. Energy flow inside a building with various types of converters that may be utilized to implement dynamic energy filtering.

[1]Yue Cao, John A. Magerko III, Thomas Navidi, and Philip T. Krein are with the Department of Electrical and Computer Engineering, University of Illinois, Urbana, IL 61801, USA (email: yuecao2@illinois.edu, magerko1@illinois.edu, navidi2@illinois.edu, krein@illinois.edu).

Frequency domain analysis is performed to illustrate such filtering potential. This analysis takes advantage of two years of data collected from solar panels and recorded at sample rates up to 5 kHz. It is important to recognize that HVAC-implemented energy resource filtering has both upper and lower frequency band limits. The lower frequency limit, meaning the lowest update rate for HVAC speed and power commands, is established to shield building users from substantial temperature swings, ideally keeping variations imperceptible. An upper frequency limit, meaning the highest update rate for HVAC speed and power commands, is needed such that the following conditions are met: 1) HVAC drives are capable of responding, 2) undue wear and tear is not induced on drives or mechanical parts, and 3) update rates do not create discomforting audible pitch or amplitude changes. Approximate frequency bounds are discussed here. These upper and lower frequency bounds complete the description in Figure 1. If the HVAC system can effectively filter power usage over a useful frequency band, the power grid would then be better able to provide and absorb slower changes power to balance the longer-term building energy flow. Any more conventional onsite energy storage could be used to balance the remainder where HVAC falls short, such as the upper frequency boundary. As a result, the power grid benefits from a much slower varied energy demand, and conventional energy storage size is substantially reduced.

A fundamental advantage of HVAC adjustment for effective dynamic thermal storage is that it is relatively easy to implement. Conventional building energy management systems and thermostats are designed to perform in slow control loops, on time scales of minutes. HVAC adjustment can use time-scale separation and stay away from this "effective dc" loop action. In this sense, an ac feed-forward signal is injected into a drive to adjust power flow on fast time scales, while avoiding interference on slow time scales. The average performance of the HVAC system remains intact, and the fast adjustment is transparent to users.

II. 5 kHz Data and Frequency Domain Analysis

Solar data have been obtained at 200 μs (5 kHz) intervals, and are used to determine energy-source-side bandwidth boundaries for an HVAC fan drive to supply dynamic energy filtering services. Details of the data are described in a separate paper [17], but the 5 kHz rate was selected to be fast enough to capture essentially all interesting solar dynamics since solar radiation and the weather do not change this rapidly. Two years of continuous data were collected from roof-mounted solar panels atop our department's building [17] during 2012-13. Two coplanar, 36-cell, photovoltaic (PV) modules (model BP SX320M) were used. Figure 2 shows the maximum power and high frequency voltage during a "noisy" day with frequent cloud cover.

The full two-year solar data set was not required to test HVAC adjustment results since representative segments could be identified to establish target bandwidths and operating dynamics. Data from three consecutive days in summer 2013 will be used here. Figure 3 shows normalized maximum solar power in per unit for this subset. Data were collected from 4 a.m. until 8 p.m. (16 hours) each day to capture all sunlight. A frequency domain analysis based on these three days is shown in Figure 4 (semi-log plot). Lower frequency components correspond to ideal diurnal solar power changes, which essentially form a "parabola" shape of daily solar profiles. Higher frequency components arise from dynamic cloud cover and similar changes. In particular, from Figure 4, frequencies lower than 1 mHz (~15 min) are associated with substantial fast Fourier transform (FFT) magnitudes. FFT magnitudes in the ~1 to ~20 mHz frequency range (~15 min to ~1 min) are likely to be suitable for local regulation with the building's thermal storage and HVAC system, since internal environmental changes at this time scale are not likely to be perceptible. Note that the FFT magnitudes in this range are 0.1% to 1%. Frequency components above about 20 mHz are nearly absent, so update rates faster than about 30 s appear to be unnecessary. Data analysis is ongoing for the entire two-year data.

With the frequency domain analysis, we model the effects of an idealized HVAC system that offsets variations by passing the solar data through various low-pass filters, each with a different cut-off frequency. In reality, this means that solar energy variation faster than a defined frequency limit is filtered by the HVAC system without being imposed on the power grid. In another words, dynamic filtering stores or releases building thermal energy via the HVAC system so that the grid sees a much smoother net energy resource, i.e., the low-pass filtered solar waveform. We use Day One from Figure 3 as an example. Figure 5 shows low-pass filtered solar panel power from this day under filters with one-, five-, fifteen-, and thirty-minute cut-off time constants normalized to the daily maximum. From Figure 5, compared with Figure 3, it appears that the filtered data with a five-, and especially fifteen-minute cut-off intervals are of primary interest for thermal storage regulation as they effectively eliminate rapid power change. Filtered data with a one-minute cut-off interval appears nearly identical to the original waveform and therefore has limited value for dynamic mitigation. Thirty-minute filtered data tends to make building users uncomfortable owing to excessive thermal swings, as will be documented later.

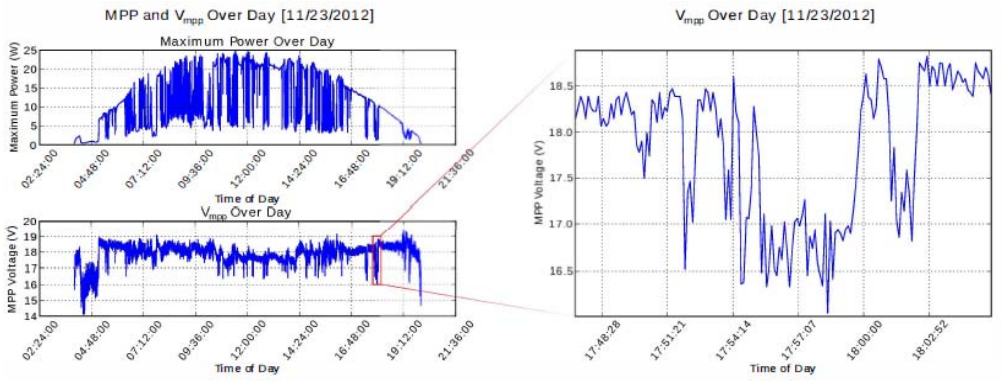

Figure 2. Illustration of 5 kHz solar data acquired on a particular day [17].

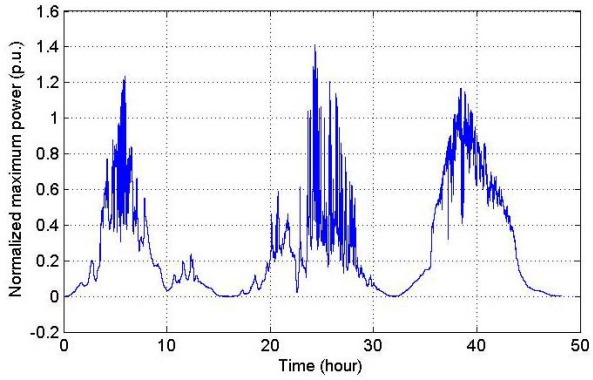

Figure 3. Solar power profile from three sampled days (4 a.m. to 8 p.m. per day).

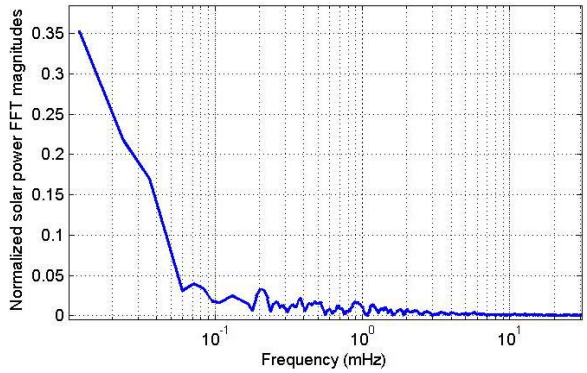

Figure 4. Day 1 solar power profile in frequency domain (log scale).

Figure 6 shows the amount of power filtered by the HVAC system under the same filter configurations as in Figure 5. The graphs represent the part of the solar energy mitigated via the building thermal energy and not by the grid. Even the one-minute cut-off interval invokes substantial energy change. As a result, our goal is to create control mechanisms for an HVAC system that effectively alleviate stochastic power up to the fifteen-minute range, or about 1 mHz. The band from 1 mHz to 33 mHz (1000 s to 30 s) appears to be of greatest interest for dynamic mitigation of solar resources. What is presented in Figure 7 is how much, in percentage, different cut-off intervals or frequencies help the grid reduce the previously necessary regulation on stochastic solar energy, given that the thermal energy is able to absorb and release this varying solar energy. From about 5% (one-minute cut-off or 17 mHz) to about 25% (fifteen-minute cut-off or 1.1 mHz) reduction, this is substantial considering the expensive operation that the grid would have burdened without such filters. One point worth mentioning is that Figure 7 does not alter average power or total energy demand from the grid. The grid-supplied total amount of energy stays the same although the grid supplies this energy much more smoothly rather than tracking rapid swings.

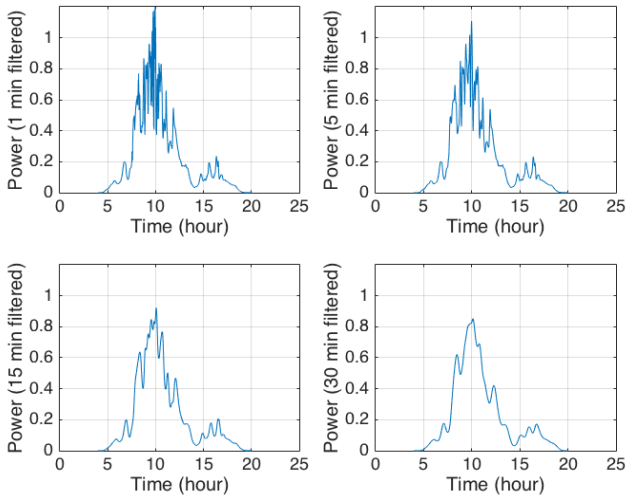

Figure 5. Solar power profile seen from the grid after HVAC filtering effect.

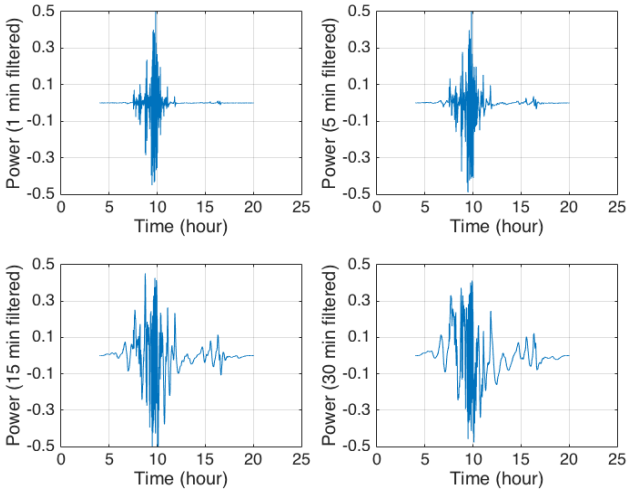

Figure 6. Solar power to be filtered by the HVAC systems.

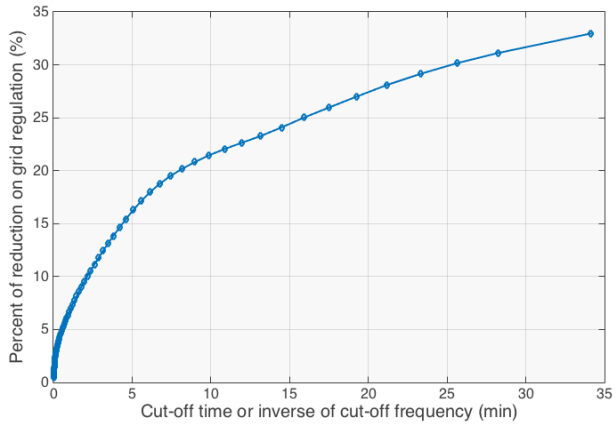

Figure 7. Percent of energy filtered for different cutoff intervals.

III. Thermal Modeling and Analysis

The following physics-based thermal model [9][18] of a commercial building is considered

$$C\frac{dT(t)}{dt} = -\frac{1}{R_w}[T(t) - T_o(t)] + c_p\dot{m}(t)[T_l - T(t)] + Q_o \quad (1)$$

where the variables and constants are described in Table I. The first term on the right hand side of the equation represents the heat loss due to heat conduction through the walls. The second term denotes the heat gain from the HVAC system. The third term is the heat gain from reheating, solar radiation, occupants, and lighting, etc., which varies depending on the time of day. The constants in Table I are estimated based on measurements obtained from a 4,000 m^2 university building [9]. Outside temperature is extracted from historic data [19]. The HVAC air flow rate is determined from a linear relationship with the fan speed, whereas the fan speed is determined from a linear relationship with the cube root of fan power. This fan power is linked with fluctuating solar power as discussed in previous sections. In this section, we assume all of the filtered solar power in Figure 6 is offset by the HVAC system. In summary, the following relationship holds:

$$\dot{m}(t) \propto \omega_{fan}(t) \propto P_{fan}^{1/3}(t) \quad (2)$$

In particular,

$$\dot{m}(t) = k_1\omega_{fan}(t) \text{ and } P_{fan}(t) = k_2\omega_{fan}^3(t) \quad (3)$$

where k_1 = 0.0964 kg/s and $k_2 = 3.3\times10^{-5}$ kW, and the nominal fan power is 35 kW [9].

A simulation based on these thermal models and parameters is run for the four filtering scenarios from Figure 6. The initial condition is assumed that the room temperature is maintained at constant 25°C if a conventional HVAC system with only grid connection is used in the building. The room temperature is now measured as stochastic solar power in Figure 6 is offset by the building thermal mass via the HVAC system. Note that a positive value in solar power means additional cooling power, thus lowering the room temperature, and vice versa. As a result, four temperature profiles are simulated and presented in Figure 8. It can be observed that there is only about ±0.5 °C and ±1.5 °C change throughout the day for the 1-minute and 5-minute cutoff filters, respectively. The ±3.0 °C change for the 15-minute cutoff filter may be pushing occupant comfort boundaries and is likely to be noticeable, while the ±8 °C for the 30-minute cutoff filter is considered too much for occupants to accept. In general, results are unique for a given building. Larger buildings with more thermal mass are likely to support 15-minute filters more readily, but the large changes for the 30-minute case may be almost insurmountable for conventional structures.

Table I. Parameter description of the thermal model.

Parameter	Description	Value
C	Building thermal capacitance	7×10^5 J/°C
$T(t)$	Building room temperature	(variable) °C
R_w	Building wall thermal resistance	5×10^{-3} °C/W
$T_o(t)$	Outside air temperature	(variable) °C
$\dot{m}(t)$	HVAC air flow rate	(variable) kg/s
c_p	Air specific heat	1006 J/g/°C
T_l	HVAC cooling air temperature	12.8 °C
Q_o	Heat gain	max 2.3×10^4 W

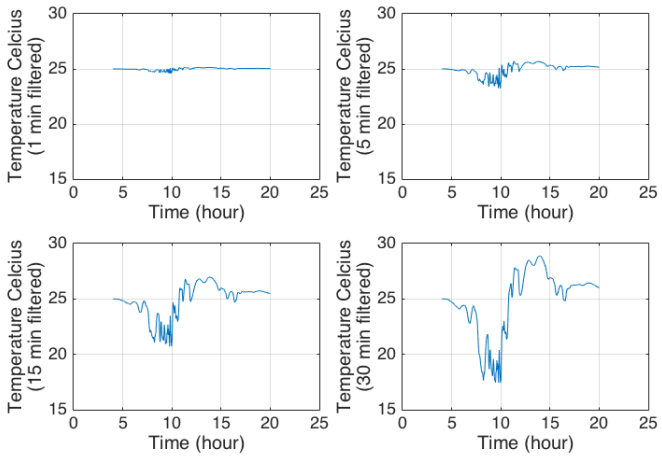

Figure 8. Room temperature profile for different filtering scenarios.

IV. Fan Drive Experiments and Discussion

To demonstrate and validate the potential of an HVAC system to filter energy content, a small fan drive was used to follow scaled responses to various band-limited solar power profiles. Results were fed into a full-scale model to determine filtering potentials. Acoustic effects of the fan drive were recorded with a high-fidelity microphone to test whether machine speed update rates cause distracting sounds. Figure 9 shows the experimental set up. A 1/3 HP, three-phase, four-pole, induction machine was coupled with a fan blower. A Yaskawa CIMR-F7U23P7 drive was used to control the fan speed through frequency and voltage. The drive was externally

programmed by a TI MSP430 microcontroller to adjust fan speed with a 0.02 s update rate to follow the solar power profiles with high fidelity.

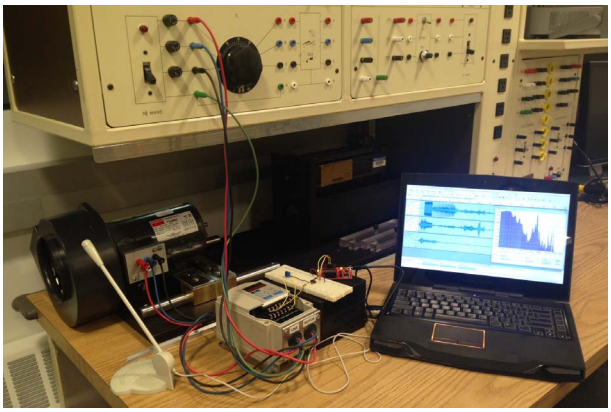

Figure 9. Experiment setup for acoustic effect from various fan speeds.

The solar power used for the audio analysis was a sample from Day 1 spanning approximately 1 min starting at 10:00 AM. We chose this sample because it includes a mix of relatively constant (±3%) and rapidly-varying (±20%) power. The data were filtered between 20 Hz and different lower frequency bounds. The lower frequency cut-off took four forms: the inverse of each 1-, 5-, 15-, and 30-minute cut-off interval. After passing the solar profile through one of these four band-stop filters, e.g., blocking 20 Hz though 1.1 mHz, the result was subtracted from the original solar data to obtain the power to be offset by the HVAC system.

This test scenario has two problems: 1) HVAC systems have maximum and minimum power capabilities. They can neither generate power nor operate above a certain power/speed threshold. We chose a maximum of ~150% of baseline speed or 86.3 Hz in this case. 2) Blower speeds must not shift rapidly or with high amplitude to avoid acoustic impacts on building occupants. To address problem 1, the maximum and minimum clamp values were implemented for speed. Problem 2 is considerably more subjective when determining acceptable update rates, and ultimately limits the amplitude and rates of allowed changes. As justified by the later acoustic tests, a ramp rate of 9 Hz/sec was chosen to be the maximum limit as this would prevent the blower from ramping between minimum and maximum speed limits in less than 10 seconds. A commanded speed profile abiding by this limitation (in addition to the hard-set max/min limit) is shown in Figure 10 along with the purely capacity-limited speed profile. Note that in Figure 10 the minimum and maximum values in effect are 0 and ~120%. Linear frequency changes are enforced any time the desired frequency changes exceeds a 9 Hz/sec limit.

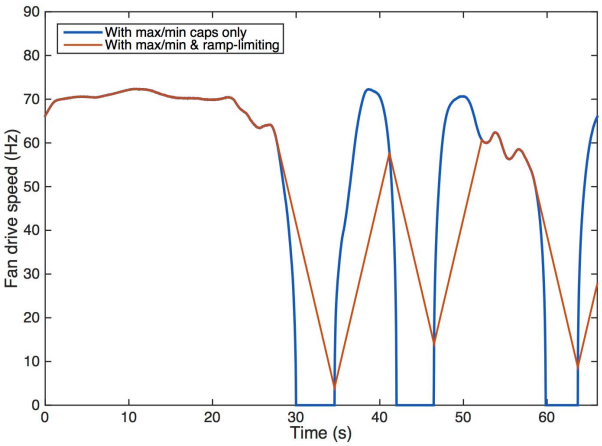

Figure 10. Commanded speed profile with speed caps and ramp-limiting.

The scenario to be tested is for a building in which 50% of the average power comes from solar. About 45% of this average load is assigned to the HVAC system [15], with a cubic relationship between speed and power. The implication is that even full modulation of an HVAC system will not be able to filter 100% of solar energy variation. However, for buildings with solar complements reaching 10-30% of the average load, HVAC dynamic adjustment might be able to manage nearly all solar variability.

In Table II, a summary of capabilities for different building types with solar installations ranging from 25% to 100% of average building load is presented with further analysis to follow. A one-minute sample of this power curve is depicted in Figure 11 in gray. The maximum and minimum filtering capabilities of Table II were found by integrating the area under the blue and gray curves and then finding the ratio between the two. The ramp-limited case is more complicated because, as observed in Figure 11, the power consumption represented by the orange curve is effectively time-delayed relative to the ideal filter. Thus during periods of rapid power fluctuation, there are times during which the HVAC filter is counterproductive. Table II confirms this unfortunate side effect with ramp-limited filtering percentages that are strictly less than the capacity limited case. The general take-away from Table II is that while the ideal HVAC filter increases in effectiveness with narrower band filters, realistic implementations including ramp limiting controls better coincide with utility company aspirations of longer periods (30 or 15 minutes) of more constant power [20]. The missed or unfiltered energy, on the other hand, has to rely on other onsite energy storage devices as mentioned in Section I. The far right column in Table II is reserved for discussion later in the paper regarding minimum and maximum fan speeds constraint.

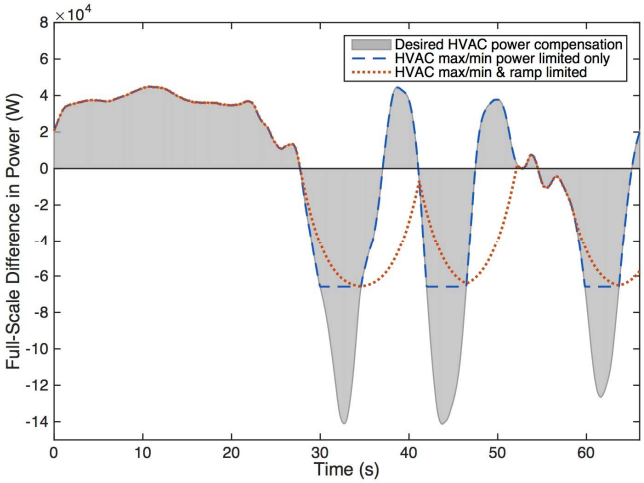

Figure 11. Desired power compensation requested from full-scale HVAC systems with and without speed clamps and ramp limiting.

Table II. Filtering capability percentage compared to ideal HVAC filter.

Solar Capacity (as % of Load)	Upper Filter Limit (period in min)	Max/min limited filtering capability	Ramp-limited filtering capability	Acoustic amplitude & ramp-rate limited capability
100	30	65.20%	62.90%	37.70%
	15	66.90%	63.90%	39.90%
	5	70.70%	65.40%	44.50%
	1	73.20%	57.90%	47.00%
50	30	83.50%	80.80%	54.40%
	15	84.70%	81.10%	56.00%
	5	85.80%	79.40%	61.00%
	1	89.50%	74.20%	62.20%
25	30	95.70%	93.40%	73.70%
	15	95.90%	93.00%	75.40%
	5	96.60%	91.70%	77.70%
	1	98.80%	92.30%	80.30%

We justify the frequency ramp-rate limit based on acoustic data by commanding four different speed profiles mentioned in Section II. These are derived from scaled power compensation requirements and fed into the MSP430 digital control. For our experiment, the fan speed and its power are related by

$$P(\omega) = 1.659\times10^{-4}\omega^3 + 2.473\times10^{-3}\omega^2 + 1.788\times10^{-2}\omega + 7.446 \quad (4)$$

where the coefficients were identified by a least squares fit as in Figure 12.

Figure 13 depicts recordings of audio samples (amplitude versus time) as well as audio from a constant 60 Hz baseline run. Each filter window shows a negative side and a positive side, which represent the amplitude changes between the motor profiles with and without ramp-limiting effects, respectively. Note that the negative side is the inverse of the magnitudes done for comparative and illustration purposes. Most noticeable in Figure 13 are the drastic changes in amplitude during a filtered profile run as well as the time delayed response in the ramp-limited case. While it may be difficult to depict visually, the difference in sound for a fan drive running at nearly 0 Hz versus nearly 90 Hz is easy to discern and potentially objectionable. Therefore, the slower, more-continuous amplitude changes observed in Figure 13 are crucial in not drawing attention to a dynamic HVAC system.

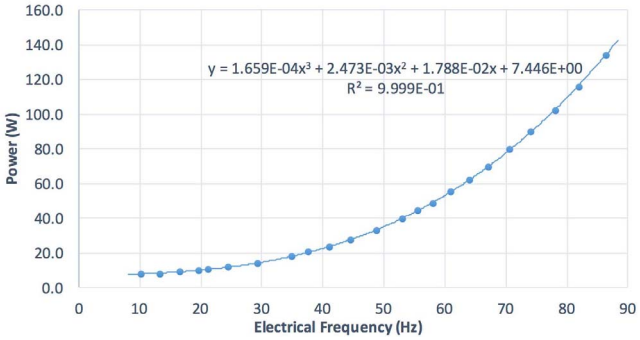

Figure 12. Small scale motor blower power vs. electrical speed.

In addition to amplitude changes, shifts in dominant audible frequencies also occur when following a filtered profile as in Section II. These dominant frequencies can originate from motor properties or structural resonances and correspond to different operating regions. Figure 14 highlights the recorded sound frequency amplitudes across the audible spectrum when moving from a high-speed "Loud" region to a low-speed "Quiet" region as designated by periwinkle and green highlights in the top part of the figure. The middle depicts the frequency content so that frequency amplitudes can be compared relative to one another. The bottom portion of Figure 14 normalizes the peak frequency amplitudes to isolate the pitches from changes in amplitude. The regions circled in blue indicate dominant frequencies that arise or become noticeably absent relative to baseline operation and would likely contribute to the conspicuousness of speed changes.

Multiple, silent, human test subjects verified that the ramp-limited profile significantly reduces the attention drawn to the blower's operation, though they admitted that the changes would still probably be distracting if occupants were to focus on them. In more realistic HVAC systems, however, motors and blowers are typically removed from the occupants, as opposed to a mere 0.5-meter away as in this experiment, hence dampening the sound of all but the changing air flow. Further tests with various ramp rates and human subjects are necessary to confirm this result, but from initial results and a subjective perspective the 0.1 Hz (10 s) frequency appears to be a plausible upper limit.

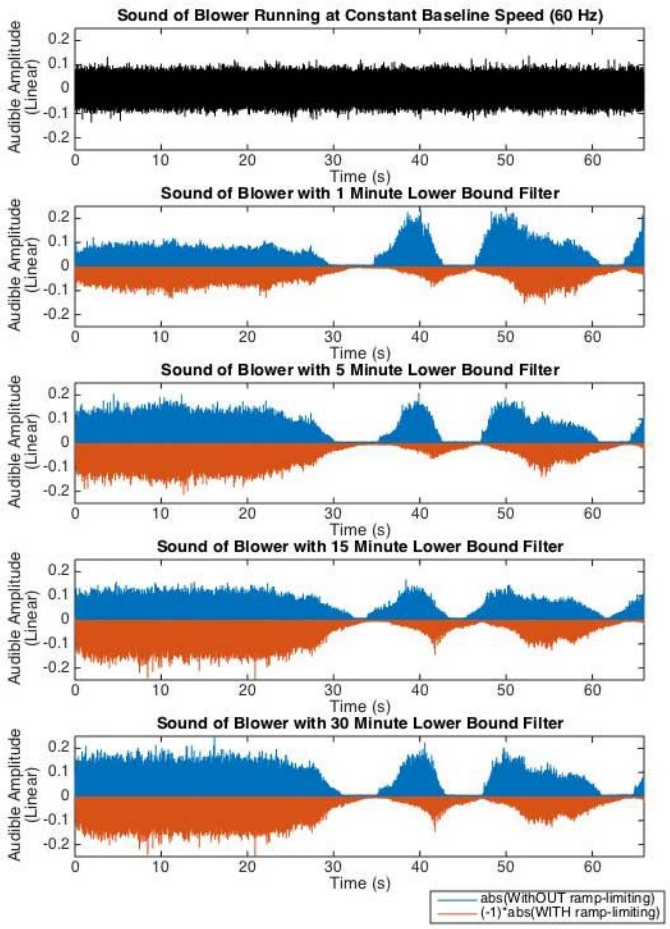

Figure 13. Fan sound in amplitude versus time for baseline case and under the 1-, 5-, 15-, and 30- minute filters.

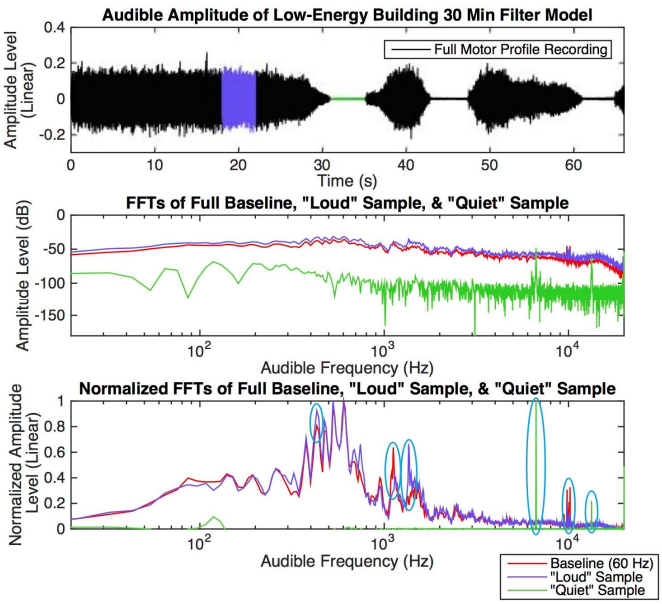

Figure 14. Sound amplitudes across audible frequency spectrum for the baseline, "Loud" sample, and "Quiet" sample.

So far we have determined how fast the blower fan speed can update without causing user discomfort, but we have not defined the absolute minimum and maximum fan speeds based on an objective of imperceptible acoustics. A series of acoustics tests, injecting one-minute sinusoidal speed commands with various amplitudes into the motor drive controller, were conducted. Taking 60 Hz as a baseline, the sinusoidal amplitudes vary ±5%, ±10%, …, ±45%. The respective recorded noise envelopes in dB are shown in Figure 15. Also shown is the peak-peak amplitude of each curve compared to the baseline magnitude to generate a normalized expectation about amplitude variations. As verified by subjective human hearing tests, the speed variation corresponding to 0 dB in Figure 15, or equivalently a peak-to-peak change equal to the baseline magnitude (±16%), seems to be imperceptible. This means that about 50 Hz and 70 Hz are appropriate minimum and maximum fan speed limits. Note that this introduces an extra constraint on the overall HVAC filtering capability, hence illustrated in the far right column in Table II.

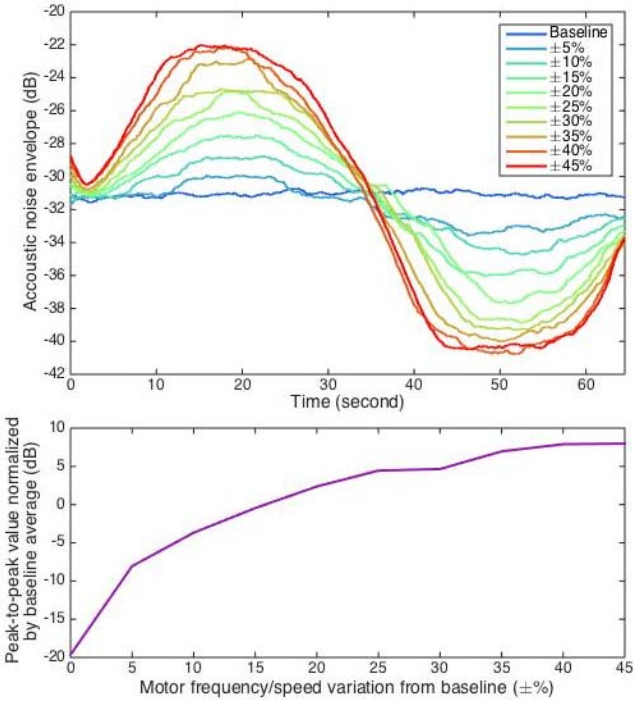

Figure 15. Acoustic noise amplitude (top) and relative amplitude change compared to baseline (bottom) for various sinusoidal fan speed profiles.

V. Conclusion and Future Work

This paper discusses a potential bandwidth for HVAC drives that allow implementation of dynamic mitigation of rapid solar energy variations. The lower update frequency limit is about 1.1 mHz (15 minutes) and seems to limit temperature variations in occupied spaces. The higher update frequency limit in the range of about 0.1 Hz (10 seconds) lets a fan respond without generating annoying noise and reduces short-term, onsite, electrical energy storage needs This is demonstrated with a small-scale fan drive experiment. Practical solar energy filtering capability by the HVAC system varies with multiple factors including installed solar capacity, fan speed ceiling, and

its ramping rates limitation. Future work will address 1) complete two-year solar data analysis to further refine the upper and lower frequency limits, 2) system-level hardware implementation with real data on an existing energy-efficient building for both thermal and acoustics studies, 3) resource look-ahead modeling for predictability in controls, and 4) calculations/experiments to determine onsite electrical energy storage capacity needed beyond existing building thermal storage, particularly for frequencies outside of our prescribed HVAC bounds.

VI. Acknowledgement

This work was supported by the Grainger Center for Electric Machinery and Electromechanics at the University of Illinois.

References

[1] X. Guan, Z. Xu, and Q. Jia, "Energy-efficient buildings facilitated by microgrid," *IEEE Trans. Smart Grid*, vol. 1, no. 3, pp. 243-252, 2010.

[2] Z. Wang, R. Yang, L. Wang, "Multi-agent control system with intelligent optimization for smart and energy-efficient buildings," in *Proc. Annual Conf. IEEE Industrial Electronics Society (IECON)*, 2010, pp. 1144-1149.

[3] T. Wei, T. Kim, S. Park, and Q. Zhu, "Battery management and application for energy-efficient buildings," in *Proc. ACM/EDAC/IEEE Design Automation Conf.*, 2014, pp. 1-6.

[4] E. Saberbari and H. Saboori, "Net-zero energy building implementation through a grid-connected home energy management system," in *Proc. Conf. Electric Power Distribution Network (EPDC),* 2014, pp. 35-41.

[5] [Online]. Available: http://news.sky.com/story/1155428/apple-campus-approved-by-cupertino-council

[6] Z. Xu, X. Guan, Q.S. Jia, and J. Wu, "Performance analysis and comparison on energy storage devices for smart building energy management," *IEEE Trans. Smart Grid*, vol. 3, no. 4, pp. 2136-2147, 2012.

[7] C.J.C. Williams, J.O. Binder, and T. Kelm, "Demand side management through heat pumps, thermal storage and battery storage to increase local self-consumption and grid compatibility of PV systems," in *Proc. IEEE PES International Conf. Innovation Smart Grid Technologies*, 2012.

[8] T. Zhou and W. Sun, "Optimization of battery–supercapacitor hybrid energy storage station in wind/solar generation system," *IEEE Trans. Sustainable Energy*, vol. 5, no. 2, pp. 408-415, 2014.

[9] H. Hao, T. Middlekoop, P. Barooah, and S. Meyn, "How demand response from commercial buildings will provide the regulation needs of the grid," in *Proc. Fiftieth Annual Allerton Conference*, 2012, pp. 1908-1913.

[10] S. Meyn, "Value and cost of renewable energy: distributed energy management," presented at the Joint JST-NSF-DFG Workshop, Honolulu, USA, 2014.

[11] J. D. Glover and F. C. Schweppe, "Advanced load frequency control," *IEEE Trans. Power Apparatus Systems*, vol. PAS-91, no. 5, pp. 2095-2103, 1972.

[12] Y. Ma, A. Kelman, A. Daly, and F. Borrelli, "Predictive control for energy efficient buildings with thermal storage: modeling, stimulation, and experiments," *IEEE Control Systems*, vol. 32, no. 1, pp. 44-64, 2012.

[13] C. Szasz, "HVAC elements modeling and implementation for net-zero energy building applications," in *Proc. IEEE International Symposium on Applied Computational Intelligence and Informatics (SACI),* 2014, pp. 195-200.

[14] P. Hernandez and P. Kenny, "From net energy to zero energy buildings: Defining life cycle zero energy buildings," *Energy and Buildings*, vol. 42, pp. 815-821, 2010.

[15] L. Perez-Lombard, J. Ortiz, and C. Pout, "A review on buildings energy consumption information," *Energy and Buildings*, vol. 40, pp. 394-398, 2008.

[16] M. Maasoumy, B. M. Sanandaji, K. Poolla, and A. Sangiovanni-Vincentelli, "Model predictive control of regulation services from commercial buildings to the smart grid," in *Proc. American Control Conf. (ACC)*, 2014, pp. 1-9.

[17] R. J. Serna, B. J. Pierquet, J. Santiago, and R. C. N. Pilawa-Podgurski, "Field measurements of transient effects in photovoltaic panels and its importance in the design of maximum power point trackers," in *Proc. IEEE Applied Power Electronics Conf.*, 2013, pp. 3005-3010.

[18] A. F. Mills, *Heat Transfer*, 2nd ed. Upper Saddle River, NJ: Prentice Hall, 1998, pp. 61-105.

[19] "Weather Underground." [Online]. Available: http://www. wunderground.com/

[20] P. Samadi, H. Mohsenian-Rad, V.W.S. Wong, and R. Schober, "Tackling the Load Uncertainty Challenges for Energy Consumption Scheduling in Smart Grid," *IEEE Trans. Smart Grid*, vol. 4, no. 2, pp. 1007-1016, 2013.